The 30th International Workshop on Water Waves and Floating Bodies, Bristol UK, April 12-15, 2015

Wave Drift Force on Floating Bodies of Cloaking Configuration and Associated Wave Patterns

Masashi Kashiwagi, Takahito Iida and Mariko Miki

Department of Naval Architecture & Ocean Engineering, Osaka University
2-1 Yamada-oka, Suita, Osaka 565-0871, Japan E-mail: *kashi@naoe.eng.osaka-u.ac.jp*

Abstract

With a semi-analytical accurate computation method and model experiment, a study is made on the phenomenon of cloaking a floating cylinder by surrounding it with a finite number of smaller circular cylinders uniformly spaced on a circle concentric with the inner cylinder. It is shown that when the optimization of the geometrical parameters of surrounding cylinders is realized to minimize the total scattered-wave energy, the wave drift force reduces to nearly zero not only on the entire bodies but also on the inner cylinder and outer surrounding cylinders individually.

1. Introduction

Cloaking phenomenon is attracting attention recently in wave-body interaction problems on the free surface. 'Cloaking' refers to the condition that there is no wave scattering in the form of radial outgoing waves. Originally this phenomenon was studied by Pendry *et al.* (2006) in electromagnetic fields. Newman (2013) has also analyzed the phenomenon of cloaking a circular cylinder of finite draft by surrounding it with an array of smaller cylinders. He has shown numerically that the scattered-wave energy can be reduced to substantially zero by optimizing the geometrical parameters of the cylinders concerned and that the mean drift force on the entire bodies becomes also very small.

The present paper is concerned with the same problem, but care is paid on the accuracy of the solution by adopting Kagemoto & Yue's theory (1986) combined with a higher-order boundary element method (HOBEM). By expressing the solution with the cylindrical coordinate system and Graf's addition theorem for Bessel functions, it is made possible to compute the wave drift force not only on the entire bodies but also on each of the bodies in the array, only in terms of the complex amplitude coefficients of scattered and incident waves. Optimization of the geometrical parameters of the cylinders is performed using the real-coded genetic algorithm (RGA) such that the total scattered-wave energy is minimized.

In order to confirm correctness of computed results, a model experiment is also conducted for an optimized configuration at the normalized wavenumber $Kd_0 = 1$ (where d_0 is the draft of the central circular cylinder), measuring the wave drift forces and also the spatial distribution of the wave elevation. It is confirmed that when the cloaking phenomenon occurs, the wave drift force becomes very small not only on the entire bodies but also on the inner cylinder and outer surrounding cylinders individually.

2. Theory for Computation

2.1 Velocity potential

We consider a number of vertical circular cylinders of finite draft (total number equal to M), specifically a central cylinder (radius r_0 and draft d_0) is surrounded by smaller $N\,(=M-1)$ cylinders of same size with radius r and draft d which are uniformly spaced on a circle of radius R_0, concentric with the inner cylinder.

To analyze multiple wave interactions among these floating bodies, the linearized potential-flow problem is considered with coordinate systems shown in Fig. 1; where in addition to the global coordinate system O-$r\theta z$ (where $x = r\cos\theta$ and $y = r\sin\theta$) fixed at the central circular cylinder, the local coordinate system O_k-$r_k\theta_k z$ is considered, with its origin placed at the center of the k-th body. The z-axis is positive vertically downward, and the plane of $z = 0$ is placed on the undisturbed free surface.

Let us consider the diffraction problem with the velocity potential expressed in the form

$$\Phi(P;t) = \mathrm{Re}\left[\frac{g\zeta_a}{i\omega}\left\{\varphi_I(P)+\varphi_S(P)\right\}e^{i\omega t}\right]. \qquad (1)$$

Here $P = (r,\theta,z)$ denotes a field point in the fluid; g is the gravitational acceleration; ζ_a and ω are the amplitude and circular frequency of an incident wave, respectively; Re means the real part to be taken.

The velocity potential of incident wave $\varphi_I(P)$, propagating in the direction with incident angle β relative to the positive x-axis, can be expressed in the cylindrical coordinate

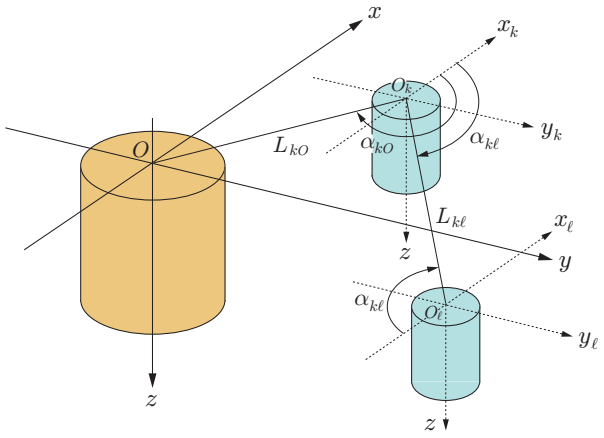

Fig. 1 Coordinate system and notations.

system as follows:

$$\varphi_I(P) = \sum_{m=-\infty}^{\infty} \alpha_m \, Z_0(z) \, J_m(k_0 r) \, e^{-im\theta} \tag{2}$$

where
$$\alpha_m = e^{im(\beta-\pi/2)}, \; Z_0(z) = \frac{\cosh k_0(z-h)}{\cosh k_0 h} \tag{3}$$

$$k_0 \tanh k_0 h = \frac{\omega^2}{g} \equiv K \tag{4}$$

with the fluid depth assumed constant and denoted as h.

The velocity potential $\varphi_S(P)$ in (1) is the scattering potential due to body disturbance. Since there are M bodies in the present analysis, it can be written as follows:

$$\varphi_S(P) = \sum_{\ell=1}^{M} \varphi_S^{\ell}(P) \simeq \sum_{\ell=1}^{M} \sum_{n=-\infty}^{\infty} A_n^{\ell} Z_0(z) H_m^{(2)}(k_0 r_\ell) \, e^{-in\theta_\ell}$$

$$= \sum_{m=-\infty}^{\infty} \mathcal{A}_m \, Z_0(z) \, H_m^{(2)}(k_0 r) \, e^{-im\theta} \tag{5}$$

where
$$\mathcal{A}_m = \sum_{\ell=1}^{M} \sum_{n=-\infty}^{\infty} A_n^{\ell} \, J_{n-m}(k_0 L_{\ell 0}) \, e^{-i(n-m)\alpha_{\ell 0}} \tag{6}$$

Evanescent wave components are ignored in (5) for brevity, and the complex amplitude of the scattered progressive wave around the ℓ-th body is denoted as A_n^{ℓ}, which is computed accurately with higher-order boundary element method (HOBEM) for computing the diffraction characteristics of elementary bodies and the wave-interaction theory of Kagemoto & Yue (1986). Here $J_m(k_0 r)$ and $H_m^{(2)}(k_0 r)$ denote the first kind of Bessel function of order m and the second kind of Hankel function of order m, respectively. The complex amplitude $\mathcal{A}_m$ in the global coordinate system, given by (6), is obtained through the coordinate transformation (see Fig. 1 for notations) and associated Graf's addition theorem for Bessel functions.

To summarize the above, the total velocity potential valid at a distance outside of all bodies can be given as the sum of (2) and (5) in the form

$$\phi(P) \equiv \varphi_I(P) + \varphi_S(P)$$

$$= \sum_{m=-\infty}^{\infty} \Big[\alpha_m J_m(k_0 r) + \mathcal{A}_m H_m^{(2)}(k_0 r) \Big] Z_0(z) \, e^{-im\theta} \tag{7}$$

For computing the wave drift force on each body, say on the ℓ-th body, we need an expression of the velocity potential valid around the ℓ-th body, in which the incident wave consists of not only the wave expressed by (2) coming from the outside but also disturbance waves due to other bodies. Thus it can be written with the ℓ-th local coordinate system in the form

$$\phi^{\ell}(P) \equiv \varphi_I^{\ell}(P) + \varphi_S^{\ell}(P)$$

$$= \sum_{m=-\infty}^{\infty} \Big[\alpha_m^{\ell} J_m(k_0 r_\ell) + A_m^{\ell} H_m^{(2)}(k_0 r_\ell) \Big] Z_0(z) \, e^{-im\theta_\ell} \tag{8}$$

where

$$\alpha_m^{\ell} = \alpha_m \, e^{-ik_0(x_{o\ell}\cos\beta + y_{o\ell}\sin\beta)} + \sum_{\substack{k=1 \\ k\neq\ell}}^{M} \sum_{n=-\infty}^{\infty} A_n^k \, H_{n-m}^{(2)}(k_0 L_{k\ell}) \, e^{-i(n-m)\alpha_{k\ell}} \tag{9}$$

and the second line in (9) is given with the coordinate transformation and associated Graf's addition theorem for Bessel functions.

2.2 Wave drift force and scattered-wave energy

According to the far-field method, the wave drift force can be computed from quadratic products of the total velocity potential valid at a distance from the body concerned. When the velocity potential is expressed with the cylindrical coordinate system, like (7) or (8), the integrals with respect to θ and z appearing in the formula by the far-field method can be analytically performed at a certain appropriate distance of r (where evanescent waves can be practically neglected), with the Wronskian relations for Bessel functions applied. After this kind of analytical integrations using (7), the calculation formula for the wave drift force on the entire bodies is given in the following complex form:

$$\frac{\overline{F}_x - i\overline{F}_y}{\frac{1}{2}\rho g \zeta_a^2 d_0} = \frac{i}{C_0 K d_0} \sum_{m=-\infty}^{\infty} \Big[2\mathcal{A}_m \mathcal{A}_{m+1}^* + \alpha_m \mathcal{A}_{m+1}^* + \alpha_{m+1}^* \mathcal{A}_m \Big], \tag{10}$$

where
$$C_0 = \frac{k_0}{K + (k_0^2 - K^2)h}. \tag{11}$$

In the same way using (8), the wave drift force on the ℓ-th body can be computed from

$$\frac{\overline{F}_x^{\ell} - i\overline{F}_y^{\ell}}{\frac{1}{2}\rho g \zeta_a^2 d_0} = \frac{i}{C_0 K d_0} \sum_{m=-\infty}^{\infty} \Big[2A_m^{\ell} A_{m+1}^{\ell *} + \alpha_m^{\ell} A_{m+1}^{\ell *} + \alpha_{m+1}^{\ell *} A_m^{\ell} \Big]. \tag{12}$$

Here the asterisk in superscript stands for the complex conjugate. It should be noted that hydrodynamic interactions among all bodies are exactly taken into account by including evanescent-wave effects in computing the complex amplitude of scattered waves, because Kagemoto & Yue's wave-interaction theory combined with HOBEM is adopted in the present theory.

Minimizing the scattered-wave energy may be used as an objective function in optimization of the parameters of outer surrounding circular cylinders. The scattered-wave energy can be computed with the same procedure as that used for computing the wave drift force. In the diffraction problem, the result can be expressed as

$$\frac{E_S}{\rho g \zeta_a^2 \frac{\omega}{k_0}} = \frac{1}{K C_0} \sum_{m=-\infty}^{\infty} \big| \mathcal{A}_m \big|^2. \tag{13}$$

3. Numerical Results

First, the real-coded genetic algorithm (RGA) was applied so as to minimize the total scattered-wave energy of all bodies, to be computed by (13), at the normalized wavenumber $K = 1$. (All parameters with length scale are nondimensionalized with the draft of central circular cylinder d_0.) Computed parameters of outer circular cylinders (r, d, R_0) are shown in Table 1; where E_S/E_{S0} denotes the energy ratio, with E_{S0} being the energy of scattered wave by the central cylinder alone.

Figure 2 shows the contour map of scattered-wave amplitude at $K = 1$ for the case of surrounding 8 bodies ($N = 8$, $M = N + 1 = 9$). It can be seen that no scattered waves exist outside of the entire bodies and almost all scattered waves are trapped between the central and surrounding bodies even for the case of $N = 8$.

Table 1 Optimized parameters of outer cylinders to minimize the total scattered-wave energy.

N	r	d	R_0	E_S/E_{S0}
4	0.2931	0.3509	2.2156	0.2948
8	0.2929	0.4834	2.2000	0.0254
16	0.1960	0.4871	2.1483	0.0199
32	0.1311	0.4506	2.1051	0.0127

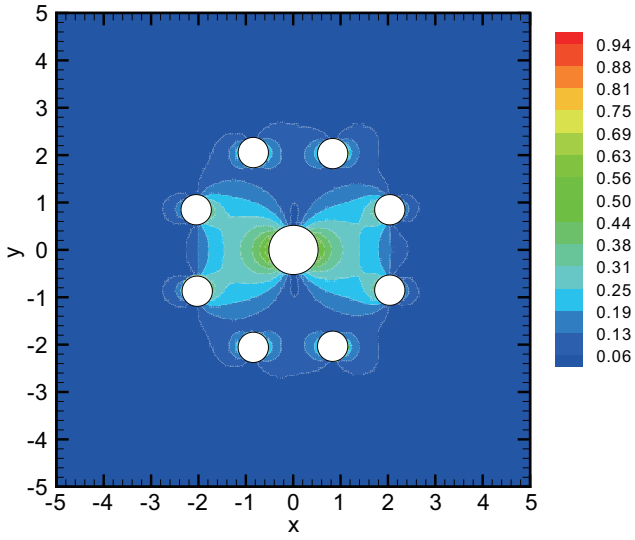

Fig. 2 Contour map of scattered-wave amplitude at $K = 1.0$ for the case of $N = 8$ shown in Table 1.

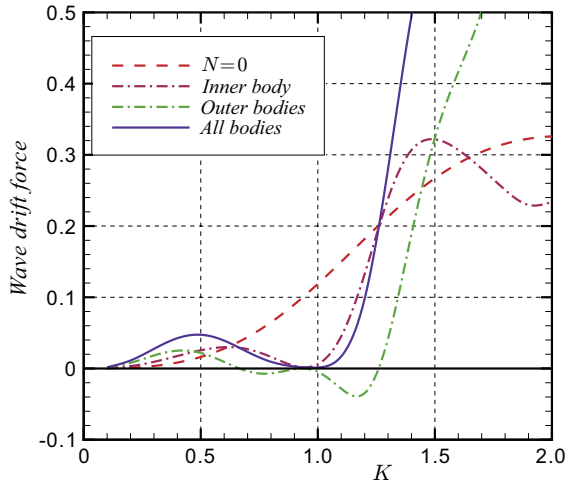

Fig. 3 Wave drift forces on the entire structure of $N = 8$ configuration and separate components acting on the inner cylinder and outer surrounding cylinders. The broken line is the force on the inner cylinder alone ($N = 0$).

The wave drift force is associated with the scattered wave, as observed by (10) and (11). However, it is not obvious whether the wave drift force becomes zero, when the scattered-wave energy of (13) is zero. Computed results for the wave drift force are shown in Fig. 3 for the case of $N = 8$. We can see at $K = 1$ that not only the force on the entire bodies (indicated by solid line) but also the individual components acting on the inner and outer bodies are also almost zero. This is because the scattered-wave pattern, shown in Fig. 2, looks symmetric with respect to the y-axis penetrating the center of inner cylinder and orthogonal to the direction of incident-wave propagation.

4. Experimental Confirmation

A model experiment has been conducted, corresponding to the numerical computations for the case of surrounding 8 circular cylinders. A photo of the model set in the wave basin is shown in Fig. 4, where the radius (r_0) and draft (d_0) of the central circular cylinder were selected as r_0 =0.134 m and d_0 =0.240 m. By referring to computed results at $K = 1$, the parameters of outer circular cylinders are selected as shown in Table 2.

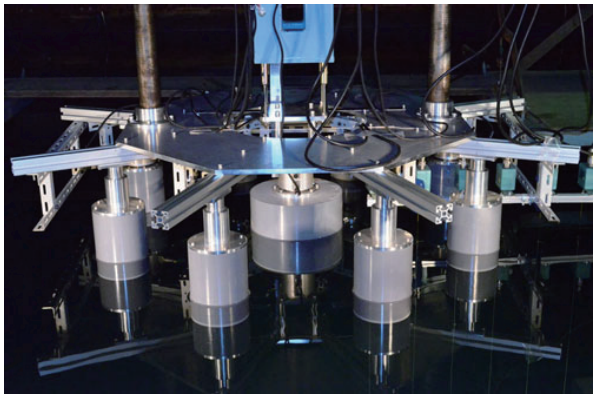

Fig. 4 Experimental model set in a wave basin.

Table 2 Parameters of outer circular cylinders used in the model experiment.

Radius	r	0.070 m	$(r/d_0 = 0.292)$
Draft	d	0.120 m	$(d/d_0 = 0.500)$
Distance	R_0	0.515 m	$(R_0/d_0 = 2.146)$

It should be noted that the length ratios shown in Table 2 are slightly different from corresponding normalized values in Table 1 for $N = 8$, on account of practical limitation in selecting materials for circular cylinders.

Although the wave elevation was measured at a number of different points, the results are shown only for the wave drift force acting on the central cylinder and also on each of outer surrounding cylinders (4 bodies due to symmetry).

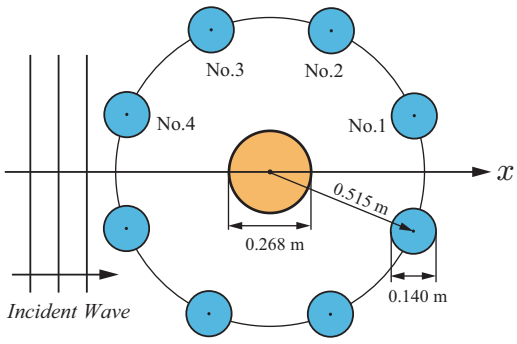

Fig. 5 Arrangement and numbering of outer cylinders.

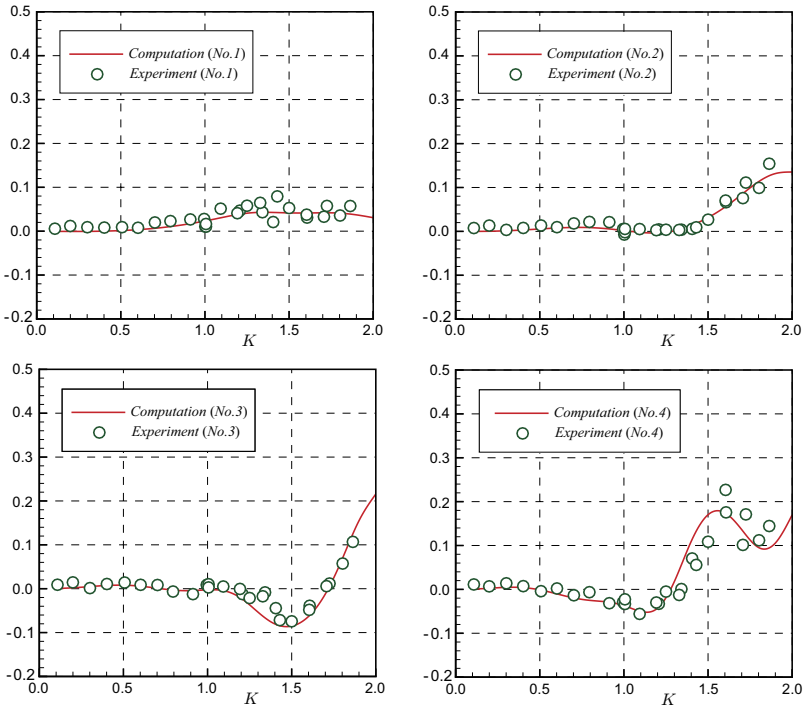

Fig. 6 Wave drift forces on each of outer cylinders (No. 1 through No. 4).

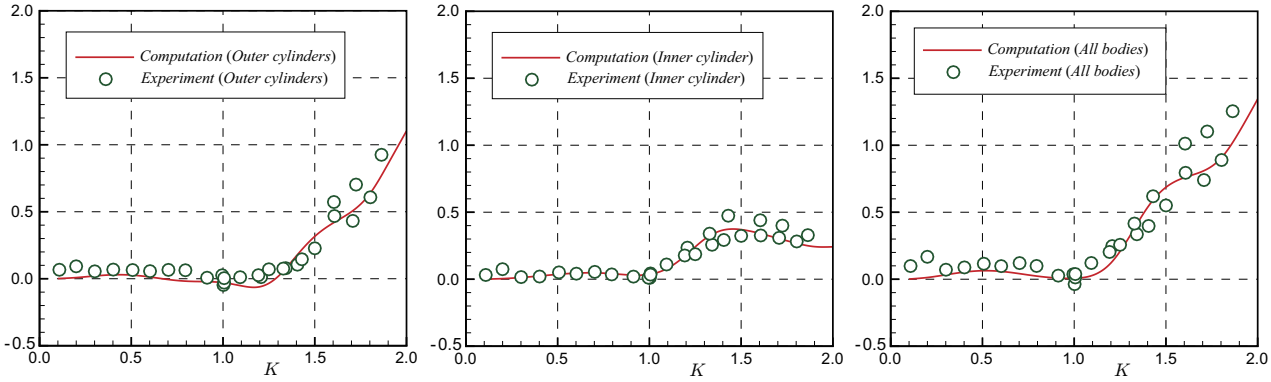

Fig. 7 Wave drift forces on outer cylinders, inner cylinder, and all cylinders.

The outer cylinders are numbered with No. 1 through No. 4 from the downwave side, as depicted in Fig. 5.

We can see in Fig. 6 relatively good agreement between computed and measured results, and at the cloaking frequency of $K = 1$ the value of No. 4 cylinder becomes negative, whereas the corresponding value of No. 1 cylinder is positive with almost the same magnitude. In fact, summing up all values acting on the outer surrounding bodies, we can obtain the result shown in Fig. 7, from which we can see that the wave drift forces on both the inner cylinder and outer surrounding cylinders are almost zero at $K = 1$.

5. Conclusions

Using a semi-analytical method with higher accuracy, the occurrence of cloaking in the surface-wave problem was confirmed for an array of smaller cylinders which surround the inner cylinder of finite draft. It was demonstrated that when the cloaking is realized, the wave drift force becomes practically zero both on the inner and outer cylinders individually. The wave pattern around the bodies was also computed and a relationship between the wave pattern and zero drift force at the cloaking frequency was noted.

Furthermore, a model experiment was conducted to confirm correctness of computed results, measuring hydrodynamic forces and the spatial distribution of the wave elevation around the bodies. Measured results for the wave elevation and their comparison with computed results will be presented at the Workshop.

References

[1] Pendry, JB, Schurig, D and Smith, DR (2006). "Controlling electromagnetic fields", *Science*, Vol 312, pp 1780–1782.

[2] Kagemoto, H and Yue, DKP (1986). "Interactions among Multiple Three-Dimensional Bodies in Water Waves: An Exact Algebraic Method", *Journal of Fluid Mechanics*, Vol 166, pp 189–209.

[3] Newman, JN (2013). "Cloaking a circular cylinder in deep water", *Proc of 28th IWWWFB* (L'Isle sur la Sorgue, France), pp 157–160.